Received: 2 April 2019 | Revised: 23 July 2019 | Accepted: 31 July 2019

DOI: 10.1111/cas.14157

ORIGINAL ARTICLE

Cancer Science WILEY

Delta-like 3 localizes to neuroendocrine cells and plays a pivotal role in gastrointestinal neuroendocrine malignancy

Kentaro Matsuo[1] | Kohei Taniguchi[1,2] | Hiroki Hamamoto[1] | Yuko Ito[3] | Sugiko Futaki[3] | Yosuke Inomata[1] | Takafumi Shima[1] | Mitsuhiro Asakuma[1] | Sang-Woong Lee[1] | Keitaro Tanaka[1] | Junji Okuda[4] | Yoichi Kondo[3] | Kazuhisa Uchiyama[1]

[1]Department of General and Gastroenterological Surgery, Osaka Medical College, Takatsuki, Japan

[2]Translational Research Program, Osaka Medical College, Takatsuki, Japan

[3]Department of Anatomy and Cell Biology, Osaka Medical College, Takatsuki, Japan

[4]Osaka Medical College Hospital Cancer Center, Takatsuki, Japan

Correspondence
Kohei Taniguchi, Department of General and Gastroenterological Surgery, Translational Research Program, Osaka Medical College, 2-7 Daigaku-machi, Takatsuki, Osaka 569-8686, Japan.
Email: sur144@osaka-med.ac.jp

Funding information
Japan Society for the Promotion of Science, Grant/Award Number: JP 18K16375; Osaka Medical College (OMC) Internal Research Grant

Abstract

Delta-like 3 (*DLL3*) is a member of the Delta/Serrate/Lag2 (DSL) group of Notch receptor ligands. Five DSL ligands are known in mammals, among which *DLL3* has a unique structure. In the last few years, *DLL3* has attracted attention as a novel molecular targeting gene in neuroendocrine carcinoma of the lung due to its high expression. However, the expression pattern and functions of *DLL3* in the gastrointestinal tract and gastrointestinal neuroendocrine carcinoma remain unclear. In this study, we examined the expression and role of *DLL3* in the gastrointestinal tract, as well as in gastrointestinal neuroendocrine carcinoma. Immunohistochemical staining of the human normal gastrointestinal tract revealed that DLL3 localized in neuroendocrine cells. DLL3 showed intense staining in chromogranin A-positive gastric cancer specimens. Real-time quantitative RT-PCR and western blotting analyses showed considerable upregulation of *DLL3* in gastrointestinal neuroendocrine carcinoma cell lines. Immuno-electron microscopy demonstrated abundant expression of DLL3 in neurosecretory granules in these cells. Furthermore, gene silencing of *DLL3* caused significant growth inhibition through the induction of intrinsic apoptosis. Our findings suggest that *DLL3* is expressed in neuroendocrine cells of the gastrointestinal tract and that it has a pivotal role in gastrointestinal neuroendocrine carcinoma cells. Based on these findings, further investigations are required to achieve a breakthrough in developing therapeutic strategies for gastrointestinal neuroendocrine carcinoma.

KEYWORDS
neuroendocrine carcinoma, apoptosis, chromogranin A, DLL3, neuroendocrine

1 | INTRODUCTION

Notch signaling influences various cellular processes, including differentiation, proliferation, survival and apoptosis.[1,2] Delta-like canonical Notch ligand 3 (*DLL3*) is a Delta/Serrate/Lag2 (DSL) Notch receptor ligand. There are 5 DSL ligands in mammals: delta-like canonical Notch ligand 1 (*DLL1*), *DLL3*, delta-like canonical Notch ligand 4 (*DLL4*), jagged 1 (*JAG1*), and jagged 2 (*JAG2*). Among these, *DLL3* is the most structurally divergent.[3] Endogenous *DLL3* localizes in the Golgi apparatus and emerges on the cell surface when overexpressed.[4] Unlike other DSL ligands, DLL3 does not bind to Notch receptors, and it inactivates Notch signaling in cis.[5] Furthermore,

DLL3 prevents the localization of Notch and *DLL1* (Notch activating ligand) to the cell surface via intracellular retainment.[6,7] Thus, *DLL3* is regarded as a cell autonomous inhibitor of Notch signaling.[3,5]

DLL3 is also expressed throughout the presomitic mesoderm and is localized to the rostral somatic compartments.[8,9] Mutations in the *DLL3* gene induce skeletal abnormalities in spondylocostal dysostosis.[10] It is reported that DLL3 is specifically expressed in the fetal brain.[11,12] Our previous findings indicated that *DLL3* expression was frequently silenced by epigenetic modifications such as aberrant DNA methylation and histone acetylation in hepatocellular carcinoma (HCC) cells,[2,13] and *DLL3* expression induced apoptosis in HCC cells.[2] Moreover, hepatitis B virus (HBV) protein (HBx) caused epigenetic modifications and suppressed the expression of *DLL3* in HBV-associated HCC.[14]

Recently, the discovery of elevated DLL3 expression on the cell surface of small cell lung cancer (SCLC) and large cell neuroendocrine carcinoma (LCNEC) cells has prompted investigation into the potential targeting of DLL3 for novel lung cancer treatments, and a DLL3-targeting antibody-drug conjugate (rovalpituzumab tesirine: Rova-T) showed tumor regression effects in SCLC and LCNEC.[12,15] These recent results suggest that *DLL3* is deeply associated with the oncological processes of NEC. However, the expression pattern and functions of *DLL3* in the gastrointestinal (GI) tract are largely unknown. In this study, we aimed to clarify the expression and roles of *DLL3* in the GI tract, including in GI-NEC.

2 | MATERIALS AND METHODS

2.1 | Patient samples

Gastrointestinal tissues were obtained from specimens following surgery at the Department of General and Gastroenterological Surgery, Osaka Medical College (Takatsuki). All samples were obtained after receiving written informed consent from the patients. This study was reviewed and approved by the institutional review board (IRB) of Osaka Medical College (acceptance number: 2535), in accordance with the tenets of the Declaration of Helsinki. The details regarding patient clinical features are shown in Tables 1 and S1.

2.2 | Cell lines, cell culture and cell viability

ECC4, ECC10 and ECC12 cells were obtained from RIKEN BRC Cell Bank (Ibaraki, Japan). ECC4 was derived from small-cell gastrointestinal carcinoma of the rectum, and ECC10 and ECC12 were derived from small-cell gastrointestinal carcinoma of the stomach. The human HCC cell line HepG2 and colon cancer cell line

TABLE 1 Pathological information of CHGA-positive gastrointestinal cancer specimens

Case	Age	Sex[a]	Site[b]	Pathology[c]	Type[d]	T[e]	N[f]	M[g]	Stage[h]	CHGA[i]
1	79	M	UMLED	por > sig, tub2	4	T4a	N2	CY1	IV	(++)
2	75	M	M	por1 > por2, sig, tub2	0-IIc	T3	N1	M0	IIB	(+) < 10%
3	73	M	M	tub2, tub1, por1 adenocarcinoma with focal neuroendocrine differentiation	0-IIc + IIa	T1b (SM 1500 μm)	N0	M0	Ia	(+)
4	77	M	UM	tub2, por	2	T3	N0	M0	IIA	(+) < 10%
5	69	M	U	Endocrine carcinoma > tub2 > por gastric mixed adenoneuroendocrine carcinoma	2	T3	N1	M0	IIB	(+++)
6	77	M	LM	Endocrine carcinoma > tub2, sig, muc, tub1 gastric mixed adenoneuroendocrine carcinoma	2	T4b	N3a	M0	IIIC	(+++)

[a]M, male; F, female.
[b]Location of tumor: D, duodenum; E, esophagus; L, lower; M, middle; U, upper.
[c]Pathological classification: por 1, poorly differentiated adenocarcinoma (solid type); por 2, (non-solid type); sig, signet-ring cell carcinoma; muc, mucinous adenocarcinoma; tub 1, well-differentiated tubular adenocarcinoma; tub 2, moderately differentiated tubular adenocarcinoma.
[d]Macroscopic classification: Type 0-IIa, superficial elevated type; 0-IIb, superficial flat type; 0-IIc, superficial depressed type; Type 1, protruded type; Type 2, localized ulcerative type; Type 3, infiltrative ulcerative type; Type 4, diffuse infiltrating type; Type 5, unclassifiable.
[e]Depth of tumor invasion: T1a, mucosa; T1b, submucosa; T2, mucosa propria; T3, subserosa; T4a, serosa exposure; T4b, serosa invasion.
[f]Lymph node metastasis (gastric cancer): N0, no metastasis; N1, 1-2 metastasis; N2, 3-6 metastasis; N3a, 7-15 metastasis; N3b, more than 16 metastasis.
[g]Distant metastasis: CY1, cytology positive; M0, no metastasis; M1, metastasis.
[h]Progress degree.
[i]CHGA, Chromogranin A.

DLD-1 were purchased from the Japanese Collection of Research Bioresources (JCRB) cell bank (Osaka, Japan). All cell lines were cultured in RPMI-1640 medium (FUJIFILM Wako Pure Chemical) supplemented with 10% FBS at 37°C under a 5% CO_2 atmosphere. The number of viable cells was determined using the Trypan blue (Life Technologies Corporation) dye-exclusion test. The other information for cell lines is shown in Data S1 as supporting materials and methods.

2.3 | Immunohistochemistry

Immunohistochemistry (IHC) was performed on 5-μm-thick formalin-fixed, paraffin-embedded tissue sections mounted on adhesive glass slides (Thermo Fisher Scientific). The slides were deparaffinized with xylene and hydrated with an ethanol series. Then, the specimens were pretreated with antigen retrieval using heat-induced epitope retrieval methods, and endogenous peroxidase was blocked by incubating the slides with 3% hydrogen peroxide. The slides were stained with the primary antibody and incubation was performed overnight at 4°C. Primary antibodies used were as follows: anti–DLL3 antibody (ab103102 1:500 dilution; Abcam) and anti–chromogranin A (code-Nr. M 0869 1:250 dilution; DAKO). Slides were then washed with PBS and then incubated with secondary antibodies (NICHIREI Biosciences) at 25°C for 1 hour; specific staining was visualized by 3,3′-diaminobenzidine (DAB) staining (NICHIREI Biosciences). Then, counterstaining with hematoxylin (MUTO PURE CHEMICALS) was performed. The specimens were inspected and photographed with an ECLIPSE 80i microscope (Nikon). Supporting experiments were performed using the same methods (Data S1).

2.4 | Double fluorescent immunohistochemistry

Following the IHC procedure described above, the slides were incubated with Protein Block Serum-Free X0909 (DAKO) for 40 minutes to block any nonspecific binding of the immunoreagents. Next, the primary anti–DLL3 antibody (ab103102 1:500 dilution; Abcam) and chromogranin A (code-Nr. M 0869 1:250 dilution: DAKO) were placed onto the same slides, and the slides were incubated overnight at 4°C. After washing in PBS, the slides were incubated with the goat anti–rabbit Alexa 488 and goat anti–mouse Alexa 594 secondary antibodies (Invitrogen Life Technologies) for 1 hour and counterstained with VECTASHIELD H1500 with DAPI (VECTOR Laboratories). They were visualized using a laser scanning microscope (Leica TCS SP8) and images were captured with LAS X software (Leica).

2.5 | Double fluorescent immunocytochemistry

Each ECC cell was seeded in a Lab-Tek II chamber slide system (Thermo Fisher Scientific) and fixed with 4% paraformaldehyde in PBS for 10 minutes, blocked for 40 minutes, and incubated with the anti–DLL3 antibody (ab103102 1:500 dilution, Abcam) and anti–chromogranin A (code-Nr. M 0869 1:250 dilution, DAKO) overnight at 4°C. Then, the results were obtained through the same processes of double fluorescent IHC described above.

2.6 | Transmission electron microscopy

Each ECC cell was harvested, rinsed with PBS, and fixed for 2 hours with 2% paraformaldehyde and 2.5% glutaraldehyde in 0.1 mol/L phosphate buffer (PB, pH 7.4), rinsed in PB, and subsequently fixed in 1% OsO_4 for 2 hours. After washing with PB, the samples were dehydrated in a series of graded ethanol, cleared in propylene oxide, and embedded in epoxy resin mixture. Thereafter, ultrathin sections (70-nm thickness) were prepared, stained with uranyl acetate and lead citrate, and examined by transmission electron microscopy (TEM) with a Hitachi-7650 (Hitachi).

2.7 | Immuno-electron microscopy

ECC4 cells were rinsed with PBS and then fixed with 4% paraformaldehyde and 0.5% glutaraldehyde in 0.1 mol/L PB (pH 7.4) for 30 minutes. After rinsing with PBS and treating the cells in 0.5% Tween 20 for 5 minutes on ice, samples were treated using the methods for IHC described above for anti–DLL3 antibody (ab103102 1:500 dilution, Abcam), fixed with 1% OsO_4 in 0.1 mol/L PB for 30 minutes, dehydrated in a series of graded ethanol, cleared in propylene oxide, and embedded in an epoxy resin mixture.

For post–embedding immunogold labeling for DLL3, ECC10 and ECC12 cells were fixed with 2% paraformaldehyde and 2.5% glutaraldehyde in 0.1 mol/L PB (pH 7.4) and 1% OsO_4 and embedded in epoxy resin mixture as in conventional TEM. Ultrathin sections (70–80 nm) were cut from epoxy-embedded cells, mounted on nickel grids, and air-dried. Ultrathin sections were etched briefly (10 minutes) with saturated sodium metaperiodate in distilled water (1 g/8 mL distilled water), followed by exposure to 0.1 N HCl. The sections were then washed in filtered, deionized water and incubated in 1% BSA in PBS for 20 minutes. After incubation with the same primary antibody (ab103102 1:50 dilution, Abcam) used in IHC for 1 hour, sections were washed several times in Tris-HCl buffer containing 0.5% Tween 20 and incubated with 5-nm, gold-conjugated anti–rabbit polyclonal antibody (British BioCell International) for 1 hour. Grids were washed and briefly stained with uranyl acetate and lead citrate by standard methods. All samples were observed by TEM (Hitachi).

2.8 | Western blotting

Whole cells were homogenized in chilled radio-immunoprecipitation assay buffer containing 25 mmol/L Tris-HCl (pH 7.6), 1% NP-40, 0.1% deoxycholic acid, 0.1% sodium dodecyl sulfate and 150 mmol/L NaCl (Thermo Fisher Scientific) with protease inhibitor cocktail (Sigma-Aldrich) and left for 15 minutes on ice. After centrifugation at 13 687 *g* for 20 minutes at 4°C, the supernatants were collected as whole-cell protein samples. Protein contents were measured with a DC Protein Assay Kit (Bio-Rad). Seven micrograms of lysate protein

were separated by SDS-PAGE using 10%-15% polyacrylamide gels (FUJIFILM Wako Pure Chemical) and then electroblotted onto a PVDF membrane (Biorad). After blockage of nonspecific binding sites with 5% nonfat milk (Cell Signaling Technology) in PBS containing 0.1% Tween 20 (PBS-T) or PVDF blocking reagent for Can Get Signal (TOYOBO), the membrane was incubated overnight at 4°C with primary antibodies, which were diluted in Can Get Signal Immunoreaction Enhancer Solution (TOYOBO). Primary antibodies used were as follows: anti–DLL3 (#2483), anti–cleaved caspase 3 (#9661), anti–cleaved caspase 9 (#9505), anti–cleaved PARP (#5625) and anti–β-actin (#3700) (Cell Signaling Technology, 1:1000). The next day, the membrane was washed with PBS-T, incubated further for 1 hour with secondary antibodies, and then washed with PBS-T. HRP-conjugated horse anti–mouse (#7076S) and anti–rabbit IgG (#7074S) (Cell Signaling Technology, 1:10 000 dilution) were used as secondary antibodies. The immunoblots were visualized by use of Immobilon Forte Western HRP Substrate (Millipore Corporation). Detection of bands was performed using FUSION-FX7 (Vilber Lourmat).

2.9 | Real-time quantitative reverse transcription polymerase chain reaction

Total RNA was extracted using NucleoSpin miRNA (MACHEREY-NAGEL) according to the manufacturer's instructions. RNA was subjected to real-time quantitative RT-PCR (RT-qPCR) with the One Step PrimeScript RT-PCR Kit (Takara Bio) on an Applied Biosystems 7500 Real-Time PCR System (Thermo Fisher Scientific). Predesigned TaqMan fluorogenic probes and primer sets for *DLL3* (Hs01085096) and *GAPDH* (Hs03929097) were purchased from Applied Biosystems (Thermo Fisher Scientific). Relative quantification of *DLL3* was normalized to the expression of *GAPDH* using the ΔΔCt method. Supporting experiments were performed using the same methods (Data S1).

2.10 | Transfection experiments

ECC4 and ECC10 cells were seeded in 6-well plates at a concentration of 1×10^5 per well on the day before transfection. Each transfection was performed by Lipofectamine RNAiMAX (Invitrogen) according to the manufacturer's protocol. The mature types of siRNA for *DLL3* (siR-DLL3; Invitrogen) were used for the transfection of the cells. Silencer Negative Control siRNA (Invitrogen) was used as a control for nonspecific effects. The sequence of siR-DLL3 #1 in this study was 5′-GACCCUCAAGGGAUUUAUGUCAUAU-3′ and that of siR-DLL3 #2 was 5′-CCGUAGAUUGGAAUCGCCCUGAAGA-3′. The effects were assessed 96 hours after transfection.

2.11 | Hoechst 33342 staining

Cells transfected with siRNA for 96 hours were detached and washed with ice-cold PBS. The cells were then stained with 5 μg/mL of Hoechst 33342 (Sigma-Aldrich) at 37°C for 1 hour, washed once with PBS, resuspended, pipetted dropwise onto a glass slide, and examined by fluorescence microscopy using a BZ-x700 (KEYENCE) equipped with an epi-illuminator and appropriate filters. The cells with condensed and/or fragmented nuclei stained with Hoechst 33342 were determined to be apoptotic. The number of apoptotic cells among 300 cells was counted.

2.12 | Caspase inhibitor experiments

Caspase inhibitor Z-VAD-FMK was obtained from Medical & Biological Laboratories. ECC4 and ECC10 cells were treated with Z-VAD-FMK for 6 hours before transfection with siR-DLL3 #2. The effects were assessed at 96 hours after transfection. Cell viability and the expression of apoptosis-related proteins were examined.

2.13 | Three-dimensional spheroid colorimetric viability assay

ECC4 cells were seeded into EZ-Bind Shunt II 96 well plates (AGC Techno Glass) at a concentration of 5×10^3 cells per well. At the same time, Silencer Negative Control siRNA or siR-DLL3 #1 and #2 (20 nmol/L) was transfected. After 96 hours of incubation, the effects were assessed by CellTiter-Glo 3D cell Viability Assay (Promega Corporation) according to the manufacturer's protocol. Luminescence was measured by GloMax-Multi+ Detection System (Promega Corporation) The photographs were taken by BZ-X700 (Keyence).

2.14 | Statistical analysis

Each examination was performed in triplicate. The statistical significance of differences was evaluated by performing the 2-sided Student's *t*-test. The values are presented as the mean ± standard deviation. A P-value < 0.05 was considered to be statistically significant.

3 | RESULTS

3.1 | The expression of DLL3 was localized to the deep layer mucosa cells in the gastrointestinal tract

First, DLL3 expression in the GI tract, including the stomach, duodenum, jejunum, ileum and rectum, was examined by IHC. Our results showed that DLL3 was expressed in the cytoplasm of the cells at the deep layer of the mucosa in the GI tract (Figure 1A-F). Chromogranin A (*CHGA*) is a representative marker of neuroendocrine cells.[16-19] Interestingly, IHC of serial tissue sections showed that the locations of DLL3 and CHGA were similar in the specimens tested (Figure 2A-E). To further clarify our findings, double fluorescence IHC was performed on tissue sections of normal stomach and duodenum. This demonstrated that the expression of DLL3 and CHGA was synchronized. In other words, DLL3 was expressed in CHGA-positive cells (Figure 3A,B).

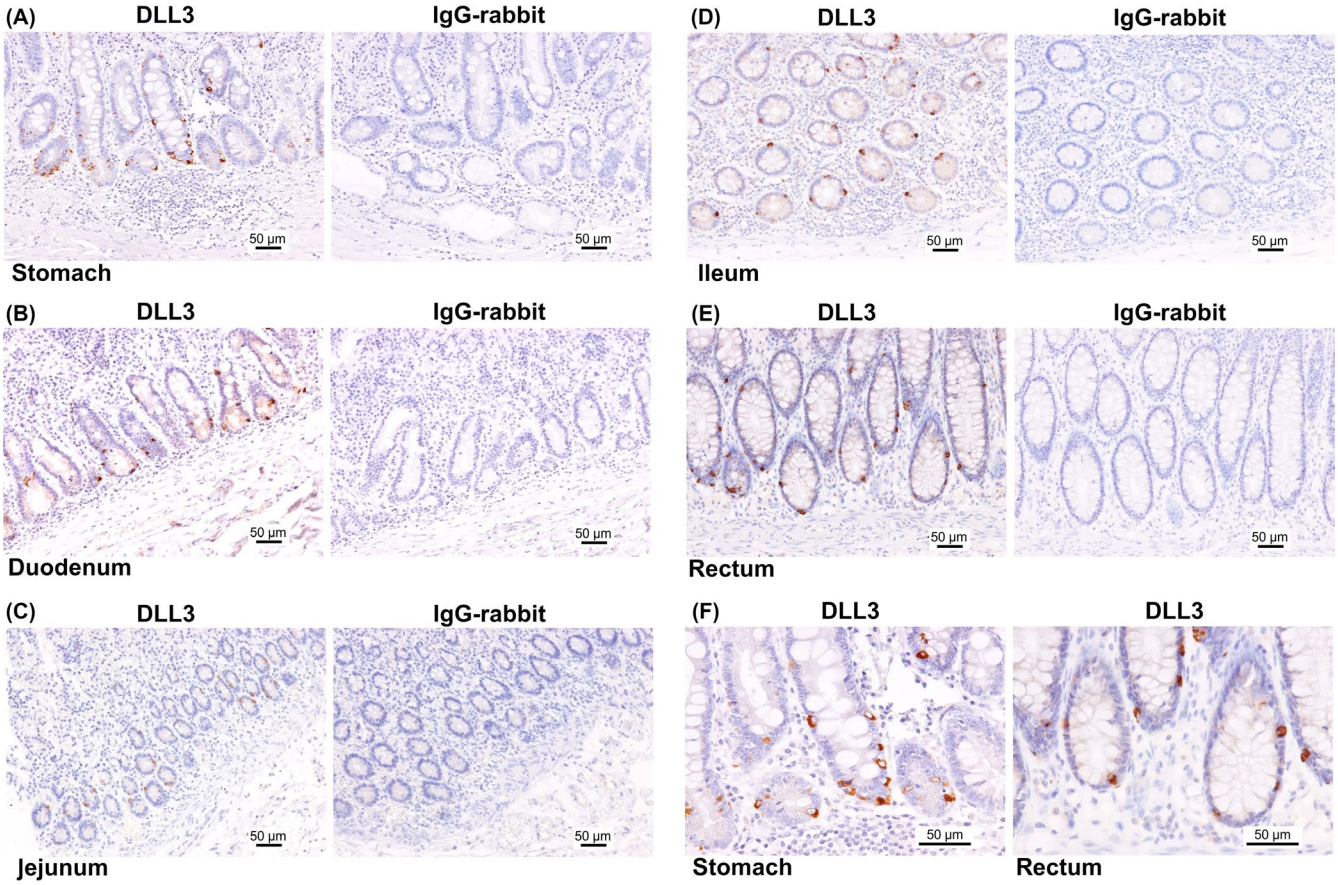

FIGURE 1 The pattern of delta-like 3 (DLL3) expression in the gastrointestinal (GI) tract. DLL3 expression in the stomach (A), duodenum (B), jejunum (C), ileum (D) and rectum (E). Left panel, the expression of DLL3; right panel, expression of IgG-rabbit used as a negative control. F, The enlarged view of (A) and (E). Scale bar: 50 μm

3.2 | DLL3 expression was associated with neuroendocrine cancer cells of gastrointestinal tract

Next, we tried to ascertain the expression of DLL3 in neuroendocrine-related GI cancer cells. Endocrine marker (CHGA)-positive gastric cancer specimens were selected (cases 1-4, Table 1). As shown in Figure 4A, DLL3 was strongly expressed in these specimens. Furthermore, DLL3 was strongly expressed in GI-NEC (mixed adenoneuroendocrine carcinoma; MANEC) specimens (cases 5 and 6, Table 1) (Figure 4A). Importantly, in the serial tissue sections of these specimens, the expression of DLL3 was positive in the CHGA-positive cancer cells (Figures 4B, S1).

3.3 | The expression levels of *DLL3* were upregulated in gastrointestinal-neuroendocrine carcinoma cells

To examine the mRNA expression level of *DLL3*, RT-qPCR was performed on GI-NEC cell lines; namely, ECC4, ECC10 and ECC12 cells. As expected, the expression levels of *DLL3* were considerably upregulated (ECC4: approximately 2000-fold, ECC10: approximately 1800-fold, ECC12: approximately 3000-fold) compared with levels in other cancer cell lines tested (Figure 5A). The same tendency was observed in the protein expression levels of DLL3 by western blot analysis (Figure 5B). Interestingly, *DLL3* mRNA expression levels of ECC cells were comparable to those of SCLC cells (Figure S2). Double fluorescent immunocytochemistry (ICC) showed that the localization of DLL3 and CHGA was similar in the cytoplasm as in the clinical specimens (Figure 6A). Interestingly, our ICC staining with electron microscopy showed that DLL3 was expressed in neurosecretory granules (Figure 6B,C).

3.4 | Knockdown of *DLL3* inhibited cell growth through the induction of apoptosis in gastrointestinal-neuroendocrine carcinoma cells

To analyze the functions of *DLL3* in GI-NEC cells, we performed gene silencing of *DLL3* in these cell lines. As shown in Figure 7A, significant growth inhibition was observed in siR-DLL3-treated GI-NEC cells. The expression levels of cleaved PARP and caspase 3 were increased in these cells (Figure 7B). Interestingly, cleaved caspase 9 expression levels, which indicate an induction of intrinsic apoptosis, were also increased (Figure 7B). Furthermore, Hoechst 33342 staining showed that the number of apoptotic cells was increased in siR-DLL3-treated ECC cells (Figure 7C). The pan-caspase inhibitor Z-VAD-FMK significantly recovered cell growth and suppressed

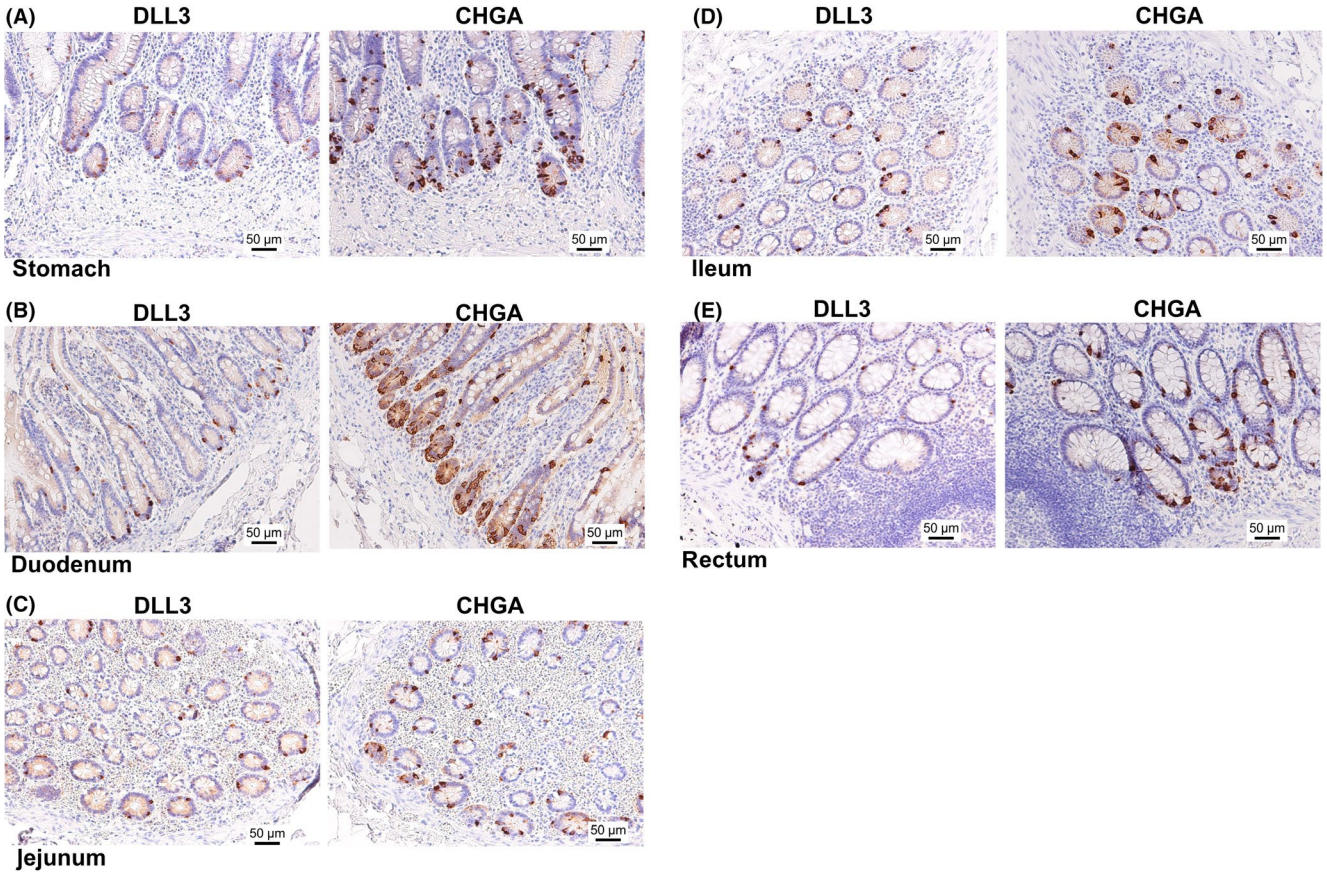

FIGURE 2 The pattern of delta-like 3 (DLL3) and chromogranin A (CHGA) expression in serial tissue sections of the GI tract. DLL3 and CHGA expression in the stomach (A), duodenum (B), jejunum (C), ileum (D) and rectum (E). Left panel, the expression of *DLL3*; right panel, expression of CHGA. Scale bar: 50 μm

the cleaved PARP expression induced by siR-DLL3 #2 (Figure 7D,E). Moreover, gene silencing of *DLL3* inhibited spheroid formation in ECC4 cells (Figure 7F,G).

4 | DISCUSSION

Previous evidence showed that *DLL3* played important roles in embryonic development.[4] In the last few years, *DLL3* has been identified as a novel therapeutic target gene, and the anti–tumor effectiveness and safety of DLL3-targeting antibody-drug conjugate (Rova-T) have been demonstrated through a clinical trial for SCLC and LCNEC.[15,20] Importantly, elevated expression of *DLL3* was detected in more than 80% of patients with SCLC.[15] Our findings in this study indicated that the considerable upregulation of *DLL3* expression was consistent even in GI-NEC cells (Figures 4,5, S2). Thus, it is possible that upregulation of *DLL3* expression universally occurs during carcinogenesis of NEC and that *DLL3* is one of the essential genes in various NEC.

In this study, we used CHGA as a positive marker of neuroendocrine cells. Granins are an acidic protein family that constitute a major component of secretory granules of various endocrine cells including neuroendocrine cells. This family is composed of 8 granin proteins (ie, chromogranin A, B, C, secretogranin (III, IV, V, VI) and VEGF).[16] Among these, CHGA is the first identified granin and is produced and excreted by granules within both endocrine glands and the diffused neuroendocrine system.[16-19] In fact, ECC cell lines used in the present study had abundant neurosecretory granules.[21] Importantly, the expression pattern of DLL3 was similar to that of CHGA in both clinical samples (Figures 2, 3 and 4) and ECC cell lines (Figure 6A), and, in particular, our immuno-electron microscopy clearly indicated that DLL3 was expressed in neurosecretory granules (Figure 6B,C). These findings support the hypothesis that *DLL3* is a novel neuroendocrine-associated gene in the GI tract (Figure 8).

In other cancers types, our group proved that *DLL3* was suppressed in HCC.[14] In contrast, the expression levels of *DLL3* were increased in pancreatic ductal adenocarcinoma.[22] Therefore, the roles of *DLL3* seem to depend on the cancer type. Interestingly, upregulation of *DLL3* was reported in cancer of the pancreas, which is one of the endocrine-related representative organs. Further investigation will clarify in detail the association between *DLL3* and neuroendocrine cells. In addition, the determination of *DLL3*-regulating mechanisms, especially in GI-NEC cells, is required.

Moreover, in NEC cells, *DLL3* knockdown might have a critical influence through the induction of intrinsic apoptosis (Figure 7). It

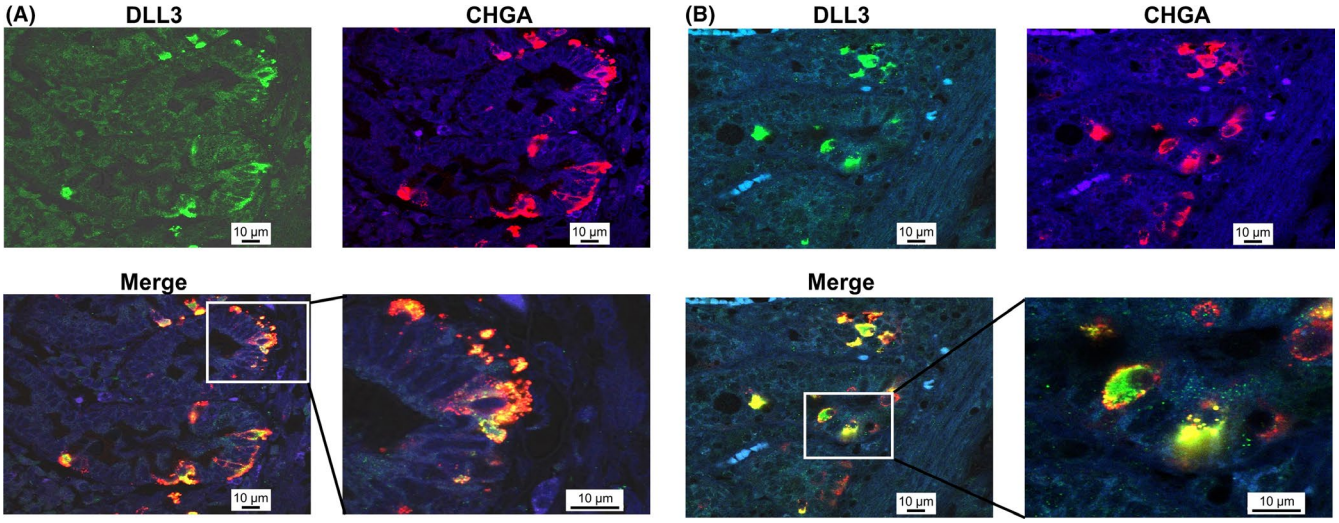

FIGURE 3 Double immunofluorescence staining of delta-like 3 (DLL3) and CHGA in normal stomach and duodenum. DLL3 and CHGA in the stomach (A) and duodenum (B). DLL3 is dyed green and CHGA red. Nuclei are dyed blue with DAPI. Lower panel, merged images, showing yellow fluorescence for co-occurring antigens. White box: enlarged area of merged view. Scale bar: 10 μm

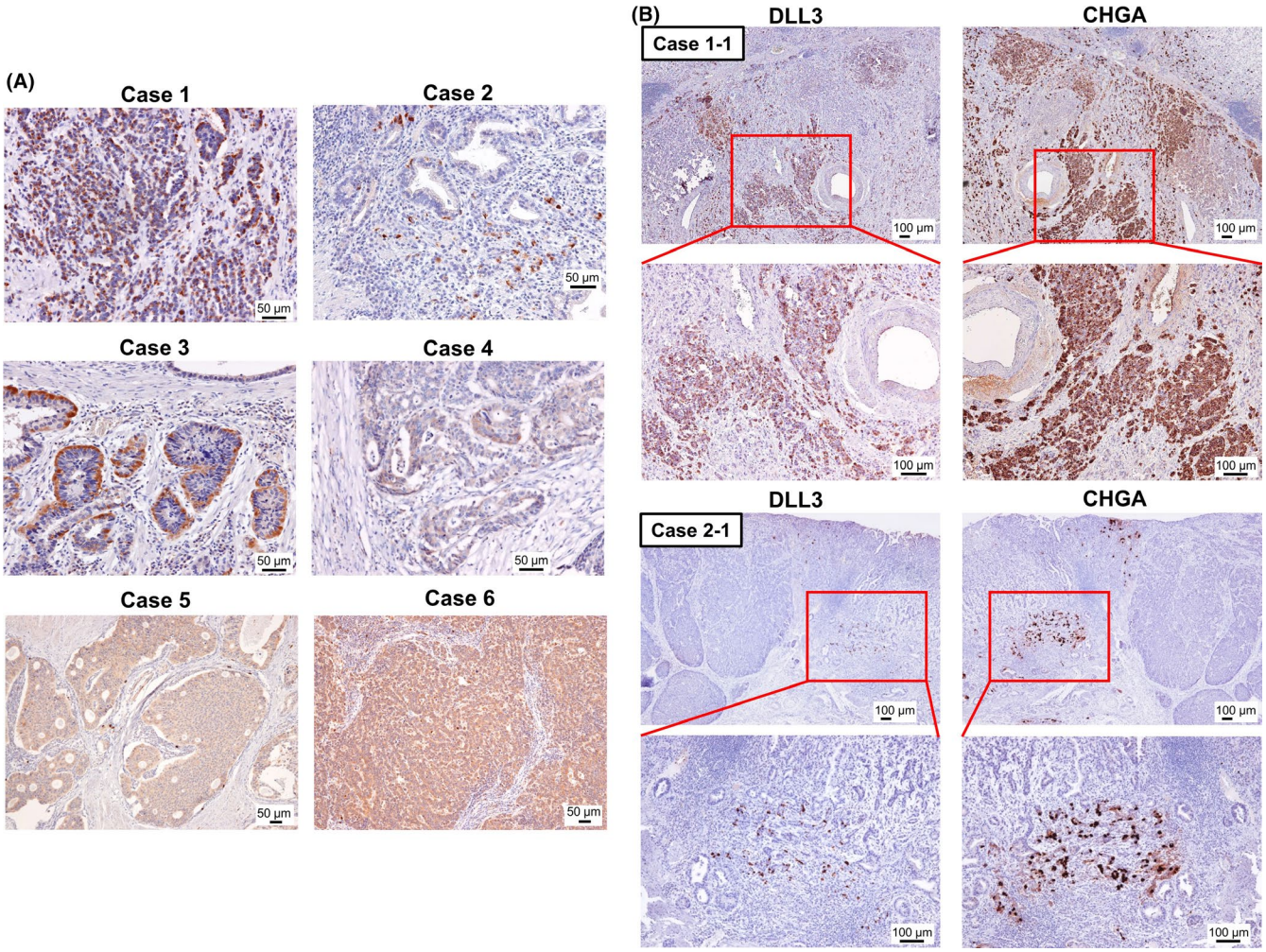

FIGURE 4 Delta-like 3 (DLL3) expression in chromogranin A (CHGA)-positive gastric cancer specimens. A, The expression of DLL3 in 4 CHGA-positive gastric cancer tissue specimens and 2 GI-MANEC tissue specimens. Detailed clinical information for each patient is shown in Table 1. Scale bar: 50 μm. B, The expression of DLL3 in a CHGA-positive area of the serial tissue sections of gastric cancer specimens. The representative images of areas of cases 1 and 2 (case 1-1 and case 2-1) are shown. Left panel, the expression of DLL3; right panel, expression of CHGA; red box, the enlarged area. The lower panel shows the enlarged versions of each image. Scale bar: 100 μm

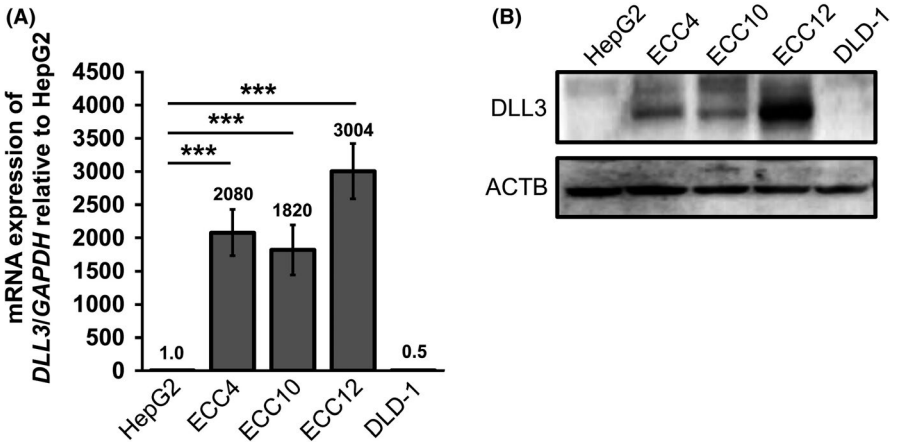

FIGURE 5 The expression levels of delta-like 3 (*DLL3*) in gastrointestinal-neuroendocrine carcinoma ECC cell lines. A, *DLL3* mRNA expression in ECC cell lines, compared with that in other cancer cell lines (hepatocellular carcinoma cells, HepG2; and colon cancer cells, DLD-1). The ratio of *DLL3* expression to that of HepG2 was calculated, and the values are shown with HepG2 normalized to 1.0. Results are presented as the mean ± SD; ***$P < 0.001$. B, The protein expression level of DLL3 in these cells

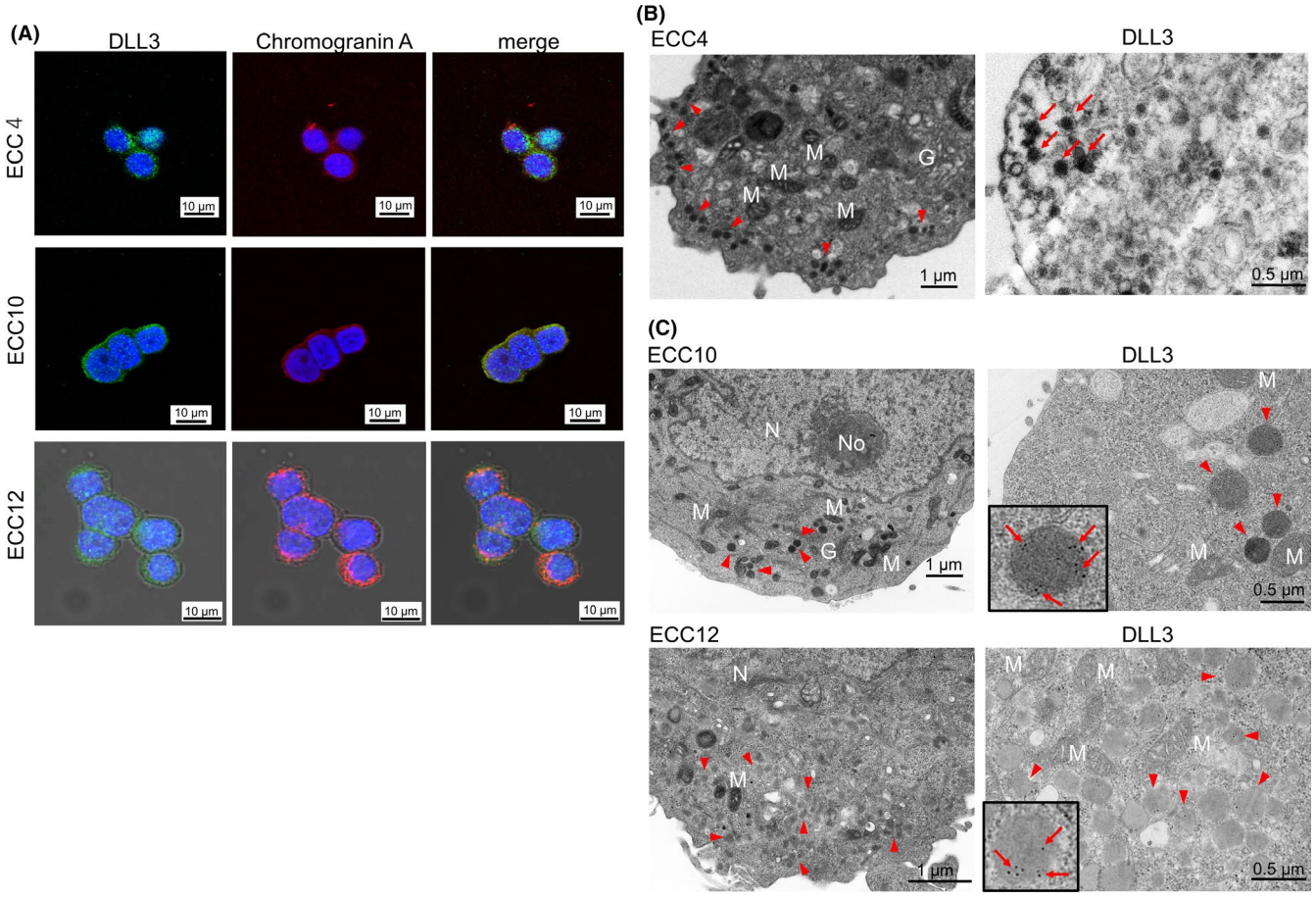

FIGURE 6 The morphological features of delta-like 3 (DLL3) expression in GI-NEC ECC cell lines. A, The immunofluorescence staining of DLL3 and chromogranin A (CHGA) in ECC4, ECC10 and ECC12 cells. DLL3 is dyed green (left panel); CHGA, red (middle panel); merged images, showing yellow fluorescence for co-occurring antigens (right panel). Nuclei are dyed blue with DAPI. Scale bar: 10 μm. B,C, The electron microscopy of ECC4, ECC10 and ECC12 cells. Left panel, transmission electron microscopy (TEM); right panel, immuno-electron microscopy of anti–DLL3 antibody. Immuno-electron microscopy for ECC4 was performed by the enzyme-labeled antibody method and that for ECC10 and ECC12 was performed by the post–embedding immuno-gold labeling method. G, Golgi apparatus; M, mitochondria; N, nucleus; No, nucleolus; red arrowhead, granules; red arrows, DLL3-positive granules. Scale bar: 1.0 μm (TEM); 500 nm (immuno-electron microscopy)

has been reported that overexpression of *DLL3* in lung carcinoma cells promoted tumor growth and reduced apoptosis.[23] Based on these findings, we conclude that *DLL3* should be considered as an essential gene for cancer cell survival in certain cancer types, including NEC (Figure 8). Of course, further investigation regarding the detailed mechanisms of induction of apoptosis by knockdown of *DLL3*

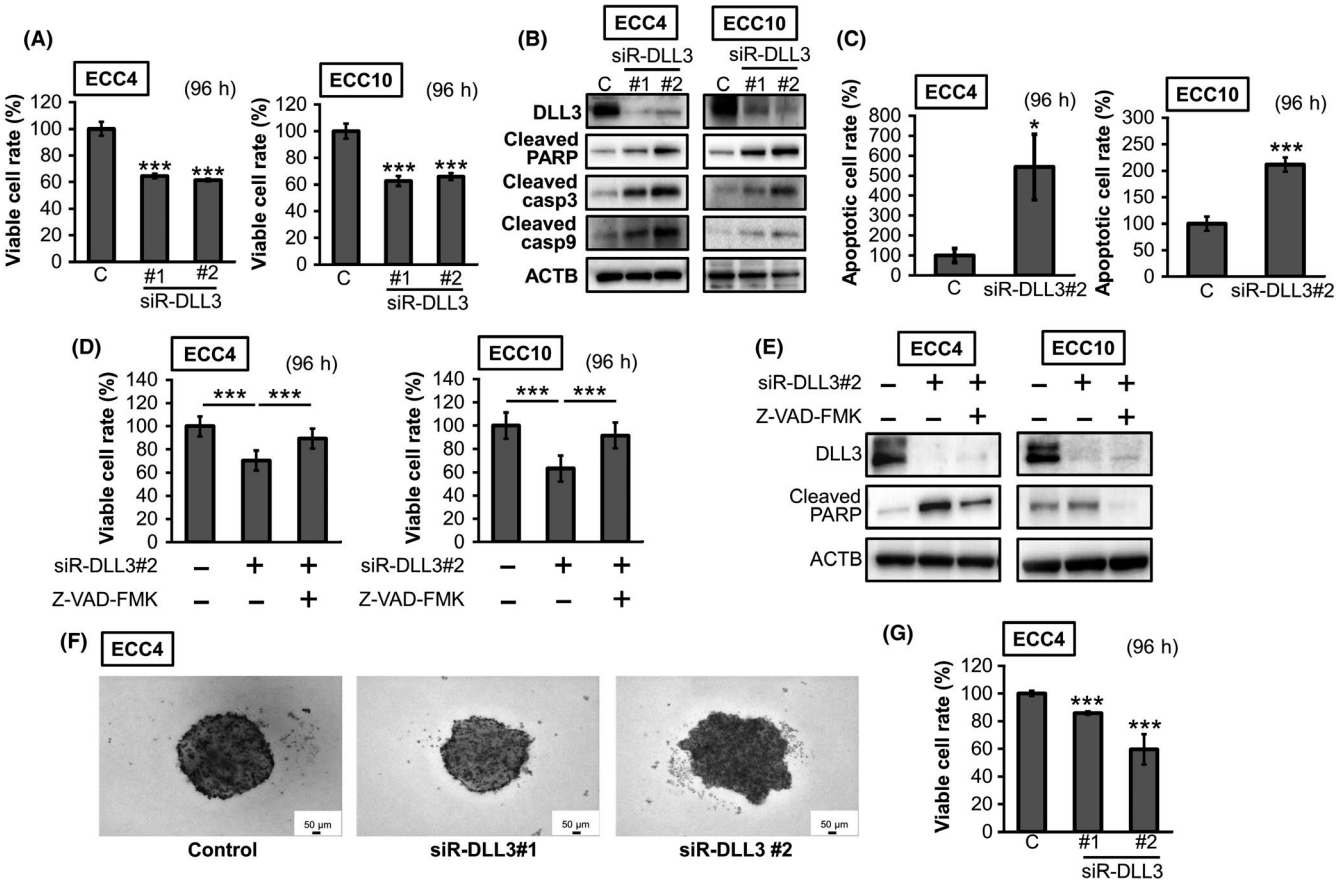

FIGURE 7 The effects of gene silencing of delta-like 3 (*DLL3*) in ECC cell lines. A, Cell viability at 96 h after transfection with siR-DLL3 (10 nmol/L). B, The protein expression levels of apoptosis-related genes. The experimental conditions were the same as in (A). C, Results of Hoechst 33342 staining. The number of apoptotic cells was counted and shown as a bar graph. The experimental conditions were the same as in (A). D, E, Apoptosis inhibition effects of Z-VAD-FMK (5 μmol/L) in ECC4 and ECC10 cells. Cells were pretreated with Z-VAD-FMK and then transfected with siR-DLL3 #2 (10 nmol/L) for 96 h. The effects on cell viability (D) and the level of cleaved PARP (E). F, G, Spheroid formation at 96 h after transfection of ECC 4 cells with siR-DLL3 (20 nmol/L) (n = 3). Representative photographs of each sample are shown (F), and the 3D cell viabilities are shown as a bar graph (G). Results are presented as the mean ± SD; * $P < 0.05$; *** $P < 0.001$

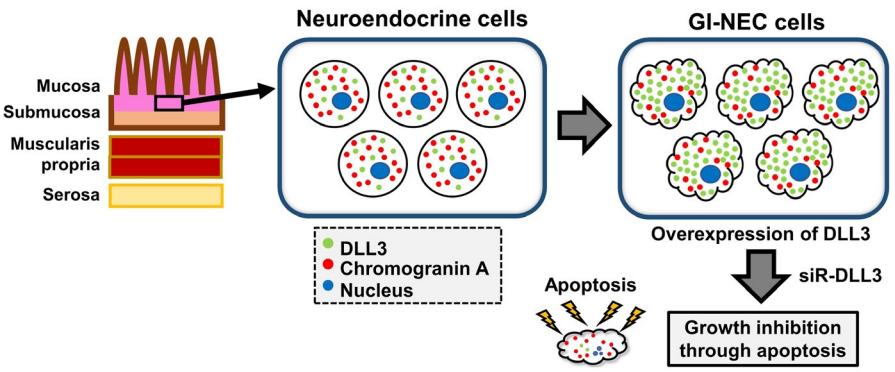

FIGURE 8 Schematic diagram of the study. Delta-like 3 (DLL3) was expressed in neuroendocrine cells of deep layer mucosa in the normal gastrointestinal (GI) tract, similar to the expression of chromogranin A (*CHGA*). Moreover, *DLL3* expression was remarkably upregulated in neuroendocrine carcinoma (NIC) cells. Importantly, gene silencing of *DLL3* caused significant growth inhibition through the induction of intrinsic apoptosis

in GI-NEC cells is necessary. In addition, the effects of ROVA-T in GI-NEC cells should be investigated in consideration of the location of *DLL3* expression.[7,24] The findings of this study may contribute to a breakthrough in therapeutic strategies for GI-NEC.

ACKNOWLEDGMENTS

We appreciate the general support given by Kentaro Maemura (former professor at the Department of Anatomy and Cell Biology,

Osaka Medical College). Furthermore, we are grateful to Akiko Miyamoto in our laboratory, Rintaro Oide (Division of Research Equipment and Devices at Osaka Medical College) and Tadashi Kanayama (Department of Anatomy and Cell Biology, Osaka Medical College). We would like to thank Editage (www.editage.jp).

DISCLOSURE

The authors have no conflicts of interest.

ORCID


Kohei Taniguchi https://orcid.org/0000-0003-0648-1370

REFERENCES

1. Radtke F, Raj K. The role of Notch in tumorigenesis: oncogene or tumour suppressor? *Nat Rev Cancer*. 2003;3:756-767.
2. Maemura K, Yoshikawa H, Yokoyama K, et al. Delta-like 3 is silenced by methylation and induces apoptosis in human hepatocellular carcinoma. *Int J Oncol*. 2013;42:817-822.
3. D'Souza B, Miyamoto A, Weinmaster G. The many facets of Notch ligands. *Oncogene*. 2008;27:5148-5167.
4. Geffers I, Serth K, Chapman G, et al. Divergent functions and distinct localization of the Notch ligands DLL1 and DLL3 in vivo. *J Cell Biol*. 2007;178:465-476.
5. Ladi E, Nichols JT, Ge W, et al. The divergent DSL ligand Dll3 does not activate Notch signaling but cell autonomously attenuates signaling induced by other DSL ligands. *J Cell Biol*. 2005;170:983-992.
6. Chapman G, Sparrow DB, Kremmer E, Dunwoodie SL. Notch inhibition by the DELTA-LIKE 3 defines the mechanism of abnormal vertebral segmentation in spondylocostal dysostosis. *Hum Mol Genet*. 2011;20:905-916.
7. Spino M, Kurz SC, Chiriboga L, et al. Cell Surface Notch Ligand DLL3 is a therapeutic target in isocitrate dehydrogenase-mutant glioma. *Clin Cancer Res*. 2019;25:1261-1271.
8. Dunwoodie SL, Henrique D, Harrison SM, et al. Mouse Dll3: a novel divergent Delta gene which may complement the function of other Delta homologues during early pattern formation in the mouse embryo. *Development*. 1997;124:3065-3076.
9. Kusumi K, Sun ES, Kerrebrock AW, et al. The mouse pudgy mutation disrupts Delta homologue Dll3 and initiation of early somite boundaries. *Nat Genet*. 1998;19:274-278.
10. Bulman MP, Kusumi K, Frayling TM, et al. Mutations in the human delta homologue, DLL3, cause axial skeletal defects in spondylocostal dysostosis. *Nat Genet*. 2000;24:438-441.
11. Loomes KM, Stevens SA, O'Brien ML, et al. Dll3 and Notch1 genetic interactions model axial segmental and craniofacial malformations of human birth defects. *Dev Dyn*. 2007;236:2943-2951.
12. Saunders LR, Bankovich AJ, Anderson WC, et al. A DLL3-targeted antibody-drug conjugate eradicates high-grade pulmonary neuroendocrine tumor-initiating cells in vivo. *Sci Transl Med*. 2015;7:302ra136.
13. Mizuno Y, Maemura K, Tanaka Y, et al. Expression of delta-like 3 is downregulated by aberrant DNA methylation and histone modification in hepatocellular carcinoma. *Oncol Rep*. 2018;39:2209-2216.
14. Hamamoto H, Maemura K, Matsuo K, et al. Delta-like 3 is silenced by HBx via histone acetylation in HBV-associated HCCs. *Sci Rep*. 2018;8:4842.
15. Rudin CM, Pietanza MC, Bauer TM, et al. Rovalpituzumab tesirine, a DLL3-targeted antibody-drug conjugate, in recurrent small-cell lung cancer: a first-in-human, first-in-class, open-label, phase 1 study. *Lancet Oncol*. 2017;18:42-51.
16. Gut P, Czarnywojtek A, Fischbach J, et al. Chromogranin A - unspecific neuroendocrine marker. Clinical utility and potential diagnostic pitfalls. *Arch Med Sci*. 2016;12:1-9.
17. Kim T, Tao-Cheng JH, Eiden LE, Loh YP. Chromogranin A, an "on/off" switch controlling dense-core secretory granule biogenesis. *Cell*. 2001;106:499-509.
18. Korse CM, Taal BG, de Groot CA, Bakker RH, Bonfrer JM. Chromogranin-A and N-terminal pro-brain natriuretic peptide: an excellent pair of biomarkers for diagnostics in patients with neuroendocrine tumor. *J Clin Oncol*. 2009;27:4293-4299.
19. Lv Y, Han X, Zhang C, et al. Combined test of serum CgA and NSE improved the power of prognosis prediction of NF-pNETs. *Endocr Connect*. 2017;7:169-178.
20. Lashari BH, Vallatharasu Y, Kolandra L, et al. Rovalpituzumab tesirine: a novel DLL3-targeting antibody-drug conjugate. *Drugs R D*. 2018;18:255-258.
21. Fujiwara T, Motoyama T, Ishihara N, et al. Characterization of four new cell lines derived from small-cell gastrointestinal carcinoma. *Int J Cancer*. 1993;54:965-971.
22. Song HY, Wang Y, Lan H, Zhang YX. Expression of Notch receptors and their ligands in pancreatic ductal adenocarcinoma. *Exp Ther Med*. 2018;16:53-60.
23. Deng SM, Yan XC, Liang L, et al. The Notch ligand delta-like 3 promotes tumor growth and inhibits Notch signaling in lung cancer cells in mice. *Biochem Biophys Res Comm*. 2017;483:488-494.
24. Furuta M, Kikuchi H, Shoji T, et al. DLL3 regulates the migration and invasion of small cell lung cancer by modulating Snail. *Cancer Sci*. 2019;110:1599-1608.

SUPPORTING INFORMATION

Additional supporting information may be found online in the Supporting Information section at the end of the article.

How to cite this article: Matsuo K, Taniguchi K, Hamamoto H, et al. Delta-like 3 localizes to neuroendocrine cells and plays a pivotal role in gastrointestinal neuroendocrine malignancy. *Cancer Sci*. 2019;110:3122-3131. https://doi.org/10.1111/cas.14157